Synthesis, Characterization and Mechanical Behaviour of Al_2O_3, TiO_2, and Cu Reinforced Al 7068 Nanocomposites

V. Sathiyarasu[1], D. Jeyasimman[2,*] and L. Chandra Sekaran[1]

[1]*Department of Mechanical Engineering, Mookambigai College of Engineering, Pudukkottai- 622502, Tamil Nadu, India and* [2]*Department of Mechanical Engineering, Periyar Maniammai Institute of Science & Technology, Thanjavur -613403, Tamil Nadu, India*

Abstract: This present research work aims at fabrication of AA7068 metal matrix composite reinforced with a different weight percentage of Al_2O_3, TiO_2 and Cu (0 wt.%, 2 wt.%, and 4 wt.%) nanopowders through mechanical alloying of 30 hrs which is produced using powder metallurgy route. The consolidation pressure of 500 MPa was applied for compaction of the composite and sintered at a temperature of 600°C for two hrs in the presence of argon gas flow. An XRD result reveals that there are no intermetallic compounds formed in the milled powder after 30 hr of mechanical alloying. The reinforcement particles were well embedded and uniformly distributed in matrix composites was confirmed by bright-field emission transmission electron microscopy (FETEM) image and selected area diffraction (SAD) ring pattern. From the DSC curve of AA 7068–2.0 wt. % Al2O3, TiO2 and Cu nanocomposite powders after 30 hrs of mechanical alloying., the endothermic peak at 536.85°C corresponds to the melting of aluminium which was followed by a steady-state exothermic reaction at 579.51°C was obtained. The green density and sintered density of prepared nanocomposites were calculated and compared. Brinell hardness test has been conducted and the maximum value of 192 BHN was obtained by adding a weight percentage of 2 wt. % of Al_2O_3, TiO_2 and Cu particles.

Keywords: Nanocomposites, Mechanical Alloying, Characterization, Mechanical Behaviour.

1. INTRODUCTION

In recent years, hybrid reinforcements with metal matrix nanocomposites are a prime consideration to enhance mechanical properties [1]. Aluminium 7068 alloy is widely used in the automotive, aerospace Industries and ordinance applications due to good mechanical properties compared with other aluminium alloys. Titanium Dioxide (TiO_2) was used as reinforcement in epoxy-co-polyamide composite and got improvement in tensile strength and elastic modulus in the recent study [2]. The effect of copper (Cu) addition in the aluminium matrix gave on the resultant hardness increment [3]. Alumina (Al_2O_3) has excellent hardness, dielectric property, wear resistance and chemical inertness properties. The effect of various reinforcements in aluminum and magnesium metal matrix composites through various synthesis methods are analysed in Table **1**.

Various authors have studied the effect of various reinforcements with aluminium metal matrix composites on mechanical properties and its microstructural analysis. However, there is limited work in the effect of hybrid reinforcement with 7068 aluminium alloy on mechanical properties and its microstructural analysis through mechanical alloying. Therefore, the main aim of the present research work is to study and investigate the effect of Al_2O_3, TiO_2 and Cu reinforced Al 7068 alloy nanocomposites through mechanical alloying on its mechanical properties and its characterization analysis.

2. EXPERIMENTAL PROCEDURE

2.1. Raw Materials

Aluminium alloy 7068 was produced by blending of highly pure (99.5 %) elemental powders and 200-mesh size. The raw materials were purchased from High Purity Laboratory Company (HPLC), India. Table **2** shows the chemical composition to make aluminium alloy 7068. Blending was done at high-energy ball mill at 250 rpm for 2 hr.

2.2. Processing of Nanocrystalline Powders

Various weight percentages (0%, 2%, 4%) of Al_2O_3, TiO_2 and Cu reinforced Al 7068 nanocomposite powders were prepared using a planetary ball mill. Balls of made up of tungsten carbide and 10 mm diameter each weighing 10 g. Totally 300 g (30 balls) were sealed with 100 g of the Al 7068 -Wt%, Al_2O_3, TiO_2 and Cu powder mixture. The speed of the mill is set to 250 rpm and the processing time is set to 30 hours. However, 5 hours of milling is alternated with 20 min. of cooling to avoid a significant temperature rise.

2.4. Compaction and Sintering

The milled powders were consolidated into cylindrical pellets of 10 mm diameter 15 mm length using a

*Address correspondence to this author at the Department of Mechanical Engineering, Periyar Maniammai Institute of Science & Technology, Thanjavur -613403, Tamil Nadu, India; Tel: +91 9486020248; E-mail: jeyasimman76@gmail.com; jeyasimmand@pmu.edu

E-ISSN: 2410-4701/20

Table 1: The Effect of Various Reinforcements in Aluminum and Magnesium Metal Matrix Composites

Sl. No	Authors	Major Metal Matrix	Reinforcements	Methods	Inferences	Ref.
1	K. Jhon Joshua *et al*.	Al 7068	-	Mechanical Alloying	AA7068 powders was reduced from 3.280 µm to 1.785 µm for a milling period of 40 hours at a speed of 101 rpm.	[4]
2	K. Jhon Joshua *et al*.	AA7068	MgO (0%, 1%, 2% and 5%)	Powder Metallurgy route	The wear resistance has been improved by adding MgO particles in AA7068 matrix material.	[5]
3.	J. Lakshmi Pathy *et al*.	AA7068 Hybrid Composites	6 vol.% of MoS2 –X vol. % of WC (X=0,5,10 and 15)	Powder Metallurgy Route	The increased wear resistant, hardness and high strength	[6]
4.	M. Madhusudhan *et al*.	AA7068	ZrO2	Stir Casting Techniques	Hardness and Tensile strength was increased with increase in Zirconium di oxide particles in weight percentage of composites	[7]
5.	V. Sridhar *et al*.	Magnesium	Al2O3 (0.35, 0.7, and 1.4 volume %)	Powder Metallurgy Route	An increase in amount of nano-alumina reinforcement led to a progressive increase in micro-hardness of pure (Mg) magnesium.	[8]
6.	Ali Hubi Haleem *et al*.	Aluminium	3, 6, 9, and 12 wt.% of α- Al2O3 particles	Powder Metallurgy Route	Improvement in Brinell Hardness (BHN) by 89% and compression strength by 54 %.	[9]
7.	M. Karbalaei Akbari	Aluminium	12 wt. % of α-Alumina nano-particles	Casting	Improvement in hardness and its tensile strength in the nanocomposites with addition of 1.5 and 2.5 vol. % Al2O3 nanoparticles	[10]
8.	M. Karbalaei Akbari	A356	Al2O3	Powder Metallurgy Route	The effect of particle size and the amount of reinforcement is given improvement in mechanical properties and fracture behavior	[11]
9.	A. Baradeswaran *et al*.	Al 7075	1.5 and 2.5 vol.% Al2O3 nanoparticles and Graphite	Liquid Metallurgy Route	Improvement in hardness and its tensile strength in the nanocomposites	[12]
10.	Chen *et al*.	Aluminium	Zn-Al-Cu-TiB2	Liquid Metallurgy Route	TiB2 content increased to 5% (mass fraction), an improvement in hardness and ultimate tensile strength (UTS) was achieved	[13]
11.	S. Dhanalakshmi *et al*.	Al7075	Al2O3-B4C	Stir Casting	The maximum tensile strength, micro-hardness and macro-hardness of 309 MPa, 140 VHN, and 112 BHN was obtained	[14]
12.	Abhishek Kumar *et al*.	A359	Al2O3	Electromagnetic Stir Casting Method	The tensile strength of the as cast composites increases on increasing the weight fraction of Al2O3.	[15]
13.	Mahallawi *et al*.	A390	Al2O3 and TiO2 nanoparticles	Mechanical Stirring	Enhancement in the micro-hardness, hardness and wear resistance of the Al2O3/TiO2 nano-dispersed hypereutectic A390 alloys	[16]
14.	A. Mazahery *et al*.	Aluminium	0.75, 1.5, 2.5, 3.5, and 5 vol. % nano-Al2O3	Mechanical Stirring	Presence of nano-Al2O3 reinforcement led to significant improvement in 0.2% yield strength and ultimate tensile stress	[17]

Table 1. contd….

Sl. No	Authors	Major Metal Matrix	Reinforcements	Methods	Inferences	Ref.
15.	Sahin *et al*.	Al 2014	Al2O3	Pow der Metallurgy Route Method	The w ear rate increased w ith increasing the load and decreased w ith increasing the particle sizes for composites	[18]
16.	S.A. Sajjadi *et al*.	A356 Aluminium Alloy	Al2O3	Stir and Compo-Casting Processes	The improvement in yield strength, ultimate tensile strength, compression strength and hardness w ere obtained	[19]
17.	S.A. Sajjadi *et al*.	A356 Aluminium Alloy	Micro and nano level Al2O3	Stirring & Compo-Casting Method	The amount of porosity in the composites increased w ith increasing w eight fraction and speed of stirring and decreasing particle size	[20]
18.	Sekar *et al*.	A356 Aluminium Alloy	Al2O3	Combined effect of Stir and Squeeze Casting	Hardness, Compressive strength and double Shear strength show ed an increase w ith an increase in addition to Al2O3 nanoparticles	[21]
19.	S. Tahamtan *et al*.	Al/A206	Nano and Micro level Al2O3	Combining ball milling and stir casting technology	Improvement in tensile properties	[22]
20.	K. Umanath *et al*.	Al 6061	SiC/Al2O3	Liquid Metallurgy Route	The w ear resistance of the 15% hybrid composite w as better than that of the 5% hybrid composite	[23]
21.	Mohammed *et al*.	Aluminium	Graphene	High energy ball milling (HEBM) & molecular level mixing (MLM) processes follow ed by spark plasma sintering (SPS)	Improvement of 79, 49 and 44% of yield strength, ultimate strength, and Vickers hardness, respectively, for 1 w t. % graphene containing nanocomposite in comparison to the unreinforced Al–4Cu alloy	[24]
22.	Avw erosuoghene Moses Okoroa *et al*.	Ti6Al4V	0.5, 1.0 and 1.5 w t% Multi-w alled carbon nanotubes (MWCNT) pow ders	High energy ball milling (HEBM) follow ed by spark plasma sintering (SPS)	Micro-hardness improved tremendously w ith an increase in sintering temperatures	[25]
23.	M. K.Akbari *et al*.	A356	TiB2 & TiO2	High Energy Ball Milling	Improvements in hardness and w ear resistance w ere obtained in A356-1.5 vol.% TiB2 composite	[26]
24.	Meysam Toozandehjani *et al*.	Al	Al2O3	High Energy Ball Milling	The increase in the milling time resulted in the homogenous dispersion of 5 w t % nanoparticles and improvement in the density, densification, micro-hardness (HV), nano-hardness (HN), and Young's modulus (E).	[27]
25.	Yilong Yang *et al*.	AA 2219	TiC	Ultrasonic Solidification	The average grain sizes of a-Al matrix alloy reduced by 61%	[28]
26.	Julia Osten *et al*.	AA 7068	5% TiC	Mechanical Alloying and Hot Pressing routes	High Strength alloy developed	[29]
27.	Amin Azimi *et al*.	Al 7068	TiC	Mechanical Alloying	High compressive strength and hardness of 938 MPa and HV 265 w ere achieved	[30]
28.	R. Taherzadeh Mousavian et. al	A356 aluminium matrix	SiC nanoparticle	Mechanical Alloying	Improvement in tensile strength (UTS), yield strength (YS) and strain	[31]

Table 1. contd....

Sl. No	Authors	Major Metal Matrix	Reinforcements	Methods	Inferences	Ref.
29.	K.R. Ramkumar *et al*.	Al 3003 alloy	TiO2 nanoparticles	Mechanical Alloying	Ultimate Tensile strength of 249 ± 04 MPa was obtained with 3% TiO2 reinforced Al 3003 composites	[32]
30.	D. eyasimman *et al*.	AA 6061	2 wt.% TiC	Mechanical Alloying	The Maximum hardness of 1180 MPa was obtained for 2 wt.% TiC.	[33]
31.	D. Jeyasimman *et al*.	AA 6061	2 wt.% MWCNT	Mechanical Alloying	The Maximum hardness of 818 MPa was obtained for 2 wt.% MWCNTs.	[34]
32.	D. Jeyasimman *et al*.	AA 6061	2 wt.% Al2O3	Mechanical Alloying	The Maximum hardness of 740 MPa was obtained for 2 wt.% Al2O3 .	[35]

Table 2: Chemical Composition of Aluminium Alloy 7068

Element	Percentage
Si	0.12
Fe	0.15
Cu	1.80
Mn	0.10
Mg	2.50
Zn	8.00
Ti	0.10
Cr	0.05
Zr	0.15
Al	Balance

hydraulic press with a capacity of 10 Tons at a compaction pressure of 500 MPa. The green pellets were sintered for 2 hours at 873 K under a reducing atmosphere and presence of the Argon gas flow. The theoretical densities of the samples were calculated using the rule of mixture. The density of sintered pellets was estimated precisely using the Archimedes principle. The estimated error in the density measurements was less than 1%.

2.5. Powder Morphology and Hardness Measurement

Nanoparticles within the Al7068 matrix was investigated by scanning electron microscopy (SEM), X-ray diffraction (XRD), transmission electron microscopy (TEM) and differential scanning calorimetry (DSC). The crystallite size and lattice strain of the milled powder samples were investigated by X-ray diffraction analysis on a D/Max Ultima III; XRD machine (Rigaku Corporation, Japan). The samples were continuously exposed to Cu Kα radiation (λ=1.5406 Å) at a scanning speed of 2° per min. operating at 30 mA and 40 KV. The scanning range was 20°-80° in steps of 0.02. The crystallite size (t) and microstrain (ε) were determined using the standard Williamson-Hall analysis [36]. The morphology of the resulting powders and distribution of reinforcement nanoparticles within the Al 7068 matrix was investigated by SEM (TESCAN model VEGA 3 LMU). The structure of mechanically alloyed powder was observed with a JOEL JEM 2100F field emission transmission electron microscope (FETEM).

3. RESULT AND DISCUSSION

3.1. Powder Morphology Evolution

The scanning electron microscope images and X-Ray diffraction peaks of the as-received pure aluminium, Al_2O_3, TiO_2 and Cu powders were shown as Fig. (**1a-d**). The aluminium powders were irregular in shape and had an average particle size of approximately 75 µm. Major peaks (1 1 1), (0 0 2), (0 2 2), (1 1 3) and (2 2 2) of aluminum with FCC crystal structures were obtained. The corresponding JCPDS Card Number is 98-008-4180. Peaks (2 1 1), (2 1 1), (0 2 1) and (1 1 3) of Al2O3 with FCC crystal structures were obtained. The corresponding JCPDS Card Number is 98-010-3822. Similarly all the eight major peaks (1 1 0), (0 1 1), (0 2 0), (1 1 1), (1 2 0), (1 2 1), (2 2 0), (0 0 2), (1 3 0), (0 3 1) and (1 1 2) of TiO2 with FCC crystal structures were obtained. The corresponding JCPDS Card Number is 98-002-2145. Three major peaks (1 1 1), (0 0 2) and (0 2 2) of Cu with FCC crystal structures were obtained. The corresponding JCPDS Card Number is 98-009-2397. As received pure powders

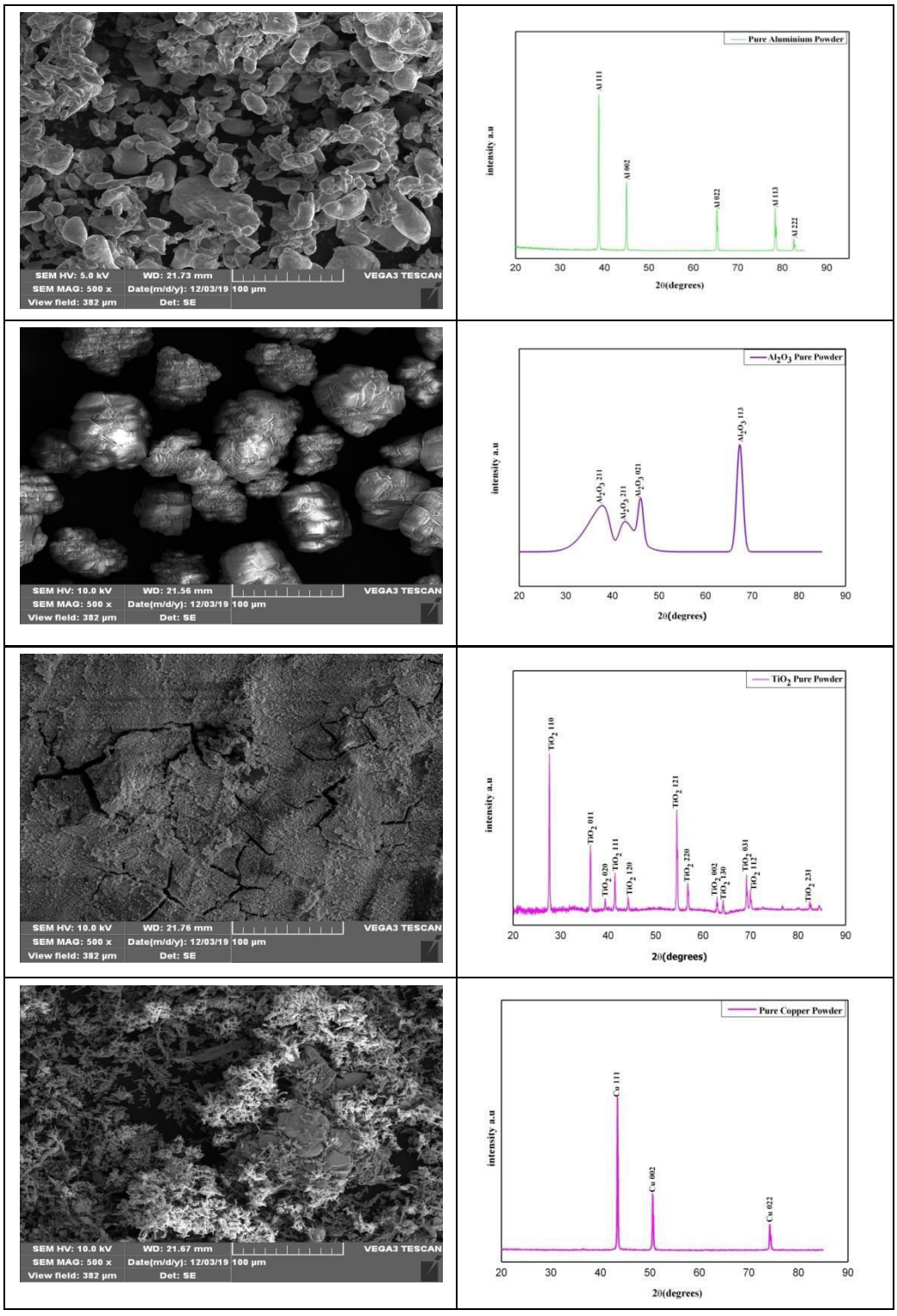

Figure 1: The SEM and XRD images of as received pure powders (a) Al (JCPDS Card Number: 98-008-4180); (b) Al2O3 (JCPDS Card Number: 98-010-3822); (c) TiO2 (JCPDS Card Number: 98-002-2415)and (d) Cu (JCPDS Card Number: 98-009-2397).

morphology and sizes were confirmed by XRD and SEM.

The aluminium 7068 powder was ball milled up to 30 hr after 5 hr ball milling was stopped and taking one-gram sample out for morphological analysis. Repeated the process up to 30 hr and kept it separate. Then aluminium 7068-2 wt. % (Al_2O_3, TiO_2 and Cu) powder particles were ball milled up to 30 hr. The mixture

powder was ball milled at 30 hr after 5 hr ball milling was stopped and taking one- gram sample out. Repeated the process up to 30 hr and kept it separate. Similarly, Aluminum 7068 -4 wt.% (Al_2O_3, TiO_2 and Cu) powder particles mixture was ball milled up to 30 hr. The mixture powder was ball milled up to 30 hr after 5 hr ball milling was stopped and taking one- gram sample out. Repeated the process up to 30 hr and kept it separate. During, ball milling the aluminium powder particle size was reduced. After the 30 hr ball milling, the microparticles changed into nanoparticles. After the 5 & 10 hr of the particle is flattening and fracturing. After 15 hr of the milling, cold welding was predo-minance. After the 20 hr of the milling, fracturing was dominance. After the 25 hr of the milling, equiaxed particle formation was started. After the 30 hr of the milling, steady state was achieved. The SEM and XRD images of Al 7068–2 Wt. % Al_2O_3, TiO_2, and Cu nanocomposite powders as a function of the milling time and its morphological changes were shown in Fig. (**2**). From the XRD images, clear peaks of Aluminum, Al_2O_3, TiO_2 and Cu were obtained and confirmed the preferred nanocomposite was Al 7068–2 Wt.%Al_2O_3, TiO_2, and Cu nanocomposite. In addition, a small Zn peak was obtained because of its weight fraction is more (7.5 Wt. %) compared to other elements in AA 7068. Peaks for Si, Mg, Fe, Ti, Cr and Mn which are related to Al 7068 alloy, were not detectable due to their low volume fraction [37]. These components were expected to dissolve in the Al lattice. Fig. (**2**), X-ray diffraction images indicate that MA decreased the peak intensities and increased the peak width of Aluminium due to the structural refinement that resulted from the MA milling time.

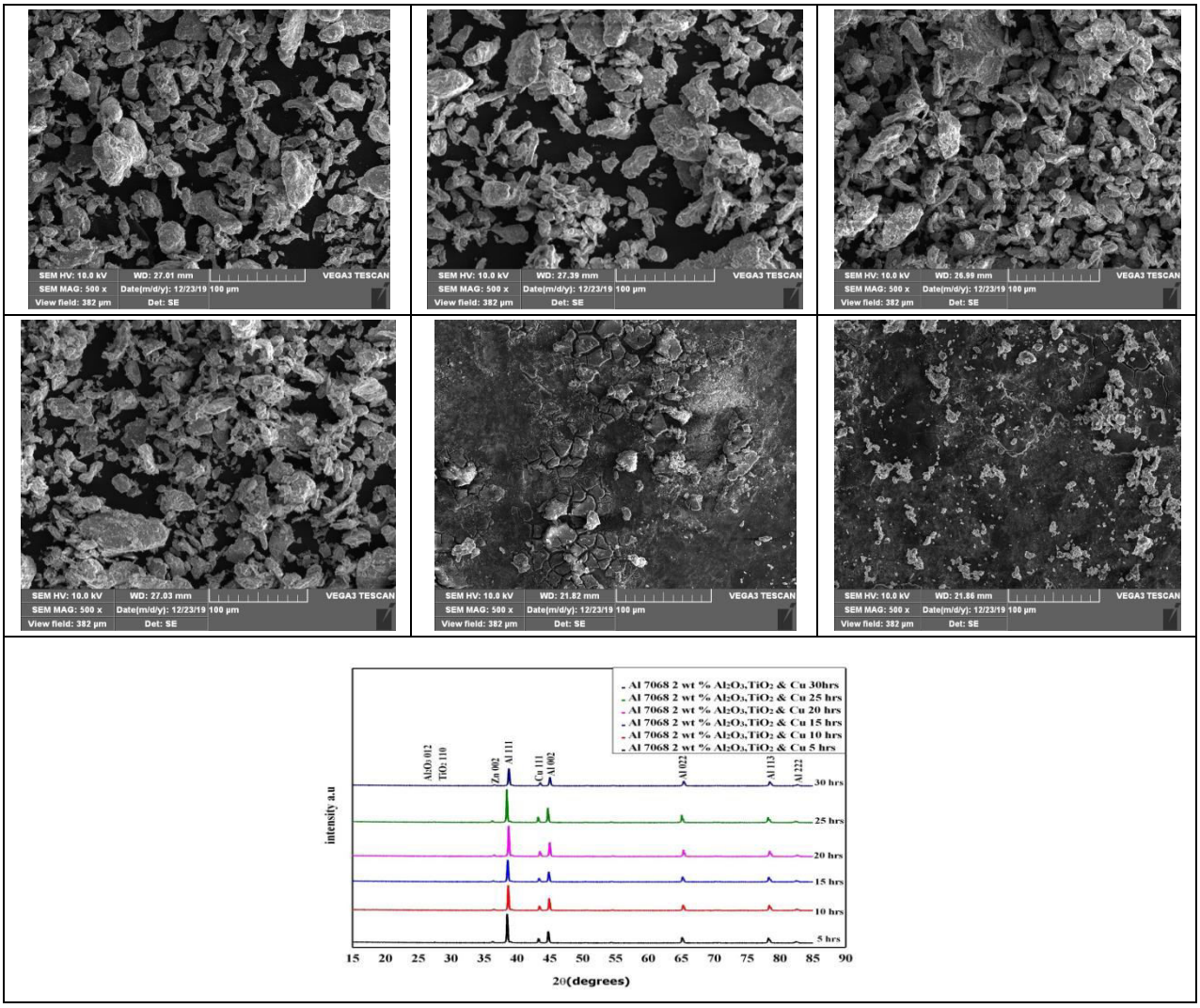

Figure 2: The SEM and XRD images of Al 7068–2 Wt.%Al_2O_3, TiO_2, and Cu nanocomposite powders as a function of the milling time after: (a) 5 h; (b) 10 h (Particle flattening and fracturing) ; (c) 15 h (Cold welding predominance) ; (d) 20 h (Fracturing dominance) ; (e) 25 h, (Equi-axed particle formation starts) and (f) 30 h (Steady state).

3.2. Structural Evaluation

Table **3** shows the structural evaluation of AA 7068 - 2wt. % Al_2O_3, TiO_2 and Cu composite powder for various mechanical alloying times (5hr, 10 hr, 15 hr, 20 hr, 25 hr and 30 hr). The crystallite size was decreased from 48 nm to 28 nm after 5 hr to after 30 hr of mechanical alloying. However, the lattice strain increased from 0.0037 to 0.005 as a function of the milling time due to the severe plastic deformation (SPD) by the high-energy ball mill. The slight decrease in the crystallite size and slight increase in the lattice strain indicate the attainment of steady state milling at 30 h. This was shown in Fig. (**3a**). The Williamson-Hall analysis [36] was adapted to measure crystallite size (t) and lattice strain (ε) using the following expression:

$$\beta_{hkl}.\cos\theta_{hkl} = \left[\frac{k\lambda}{t}\right] + 4\varepsilon.\sin\theta_{hkl} \quad (1)$$

where k is the shape factor (0.9), λ is the wavelength of the X-ray radiation (1.5406), θ_{hkl} is the Bragg angle and β_{hkl} is the full-width at half maximum after instrumental broadening correction. The first five Al reflections, peaks (1 1 1), (0 0 2), (0 2 2), (1 1 3) and (2 2 2) were used to construct a linear plot of $\beta_{hkl}\ cos\ \theta_{hkl}$ against $4\ sin\ \theta_{hkl}$. Crystallite size (t) was obtained from the intercept and the strain (ε) from the slope. The lattice parameter calculated by using interplanar spacing and miller indices. The actual lattice parameter was obtained from the intercept as described by Cullity [37] by constructing a linear plot between the calculated lattice parameter for each Bragg angle on the Y-axis and the corresponding value of $\cos^2\theta/\sin\theta$ on the X-axis. The lattice parameter reported for pure FCC Al at room temperature is 4.0496 Å [37]. The lattice parameter reported for Al 6061-2 wt. % Al_2O_3 nanocrystalline is 4.0456 Å after milling for 30 h [35]. In this investigation, the lattice parameter for the Al 7068-2 wt. % Al_2O_3, TiO_2 and Cu nanocrystalline matrix was

Table 3: Structural Characterization of AA 7068 -2wt. % Al_2O_3, TiO_2 and Cu Composite Powder for Various Ball Milling Times (hr)

Sl. No.	Ball Milling (hrs)	Crystallite Size (nm)	Lattice Strain (ε)	Lattice Parameter (a) Å	Unit Cell Volume (V) m^3
1	5	48	0.003742	4.0490	66.38092
2	10	43	0.004112	4.0480	66.33175
3	15	37	0.004571	4.0462	66.24331
4	20	34	0.004985	4.0448	66.17457
5	25	31	0.005500	4.0425	66.06175
6	30	28	0.006140	4.0410	65.98824

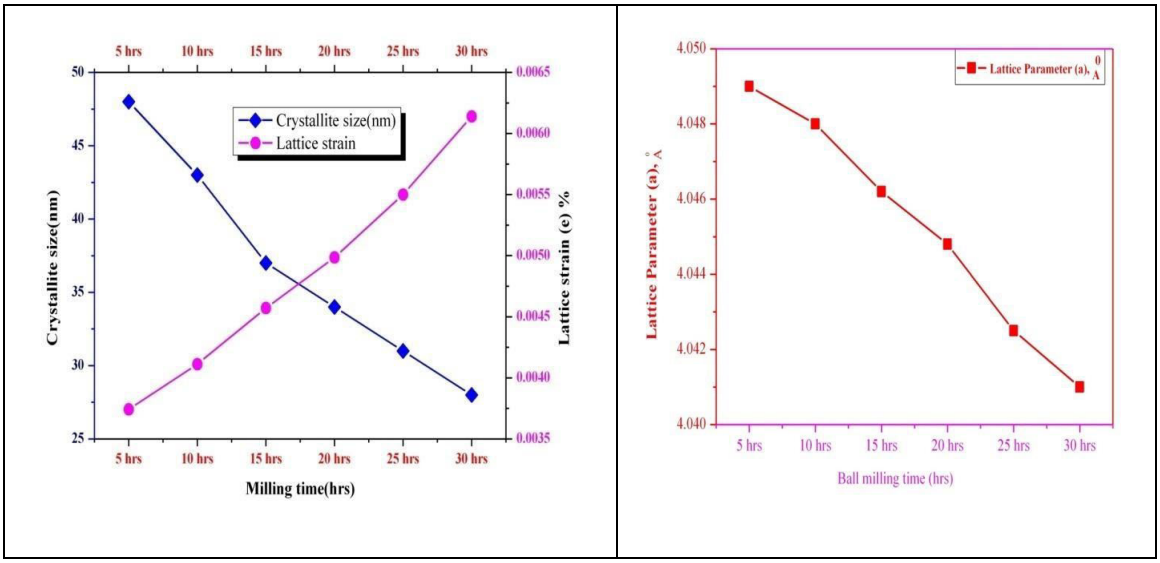

Figure 3: (a) Change in crystallite size and lattice strain of AA 7068–2 wt.% Al_2O_3, TiO_2 and Cu as a function milling time; (b) lattice parameter as function of milling time.

4.0414 Å after milling for 30 hr. So that the adding reinforcement, reduces lattice parameters values slightly.

Fig. (**4a**) shows the bright field emission transmit-ssion electron microscopy (FETEM) image of Al 7068-2 wt. % Al_2O_3, TiO_2 and Cu after 30 hr. From that image, bright areas represent nanocrystalline aluminium matrix and dark areas represent cu and TiO_2 nanoparticles. In addition, alumina nanoparticles were identified. From Fig. (**4a**), the observed grain size of the α-Al matrix is almost equi-axed and at an ultra-fine level. Further, the Al_2O_3, TiO_2 and Cu nanoparticles were uniformly distributed and embedded in the α-Al matrix. Fig. (**4b**) shows the selected area diffraction pattern and confirms the nanocrystalline composite powder.

Fig. (**5**) Shows the DSC curve of AA 7068–2.0 wt. % Al2O3, TiO2 and Cu nanocomposite powders after 30 hrs of Ball milling. DSC curve of Al 7068-2 wt.% Al2O3, TiO2 and Cu nanocomposites analysed, because The 2 wt.% of reinforcement content in metal matrix gave optimum mechanical properties (Hardness value). Hence, Al 7068-2 wt. % Al2O3, TiO2 and Cu nano-composites were taken for analysis

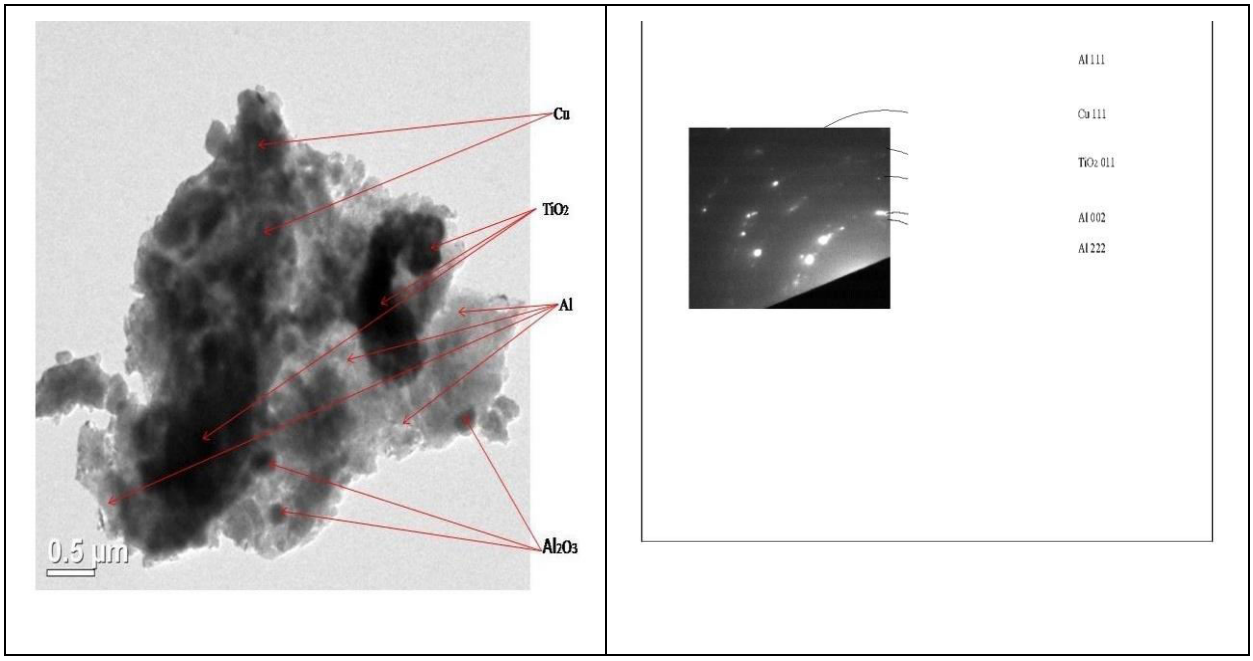

Figure 4: (a) Bright Field Emission Transmission electron microscopy (FETEM) image of Al 7068-2 wt. % Al_2O_3, TiO_2 and Cu after 30 hr; (b) Corresponding SAD ring pattern.

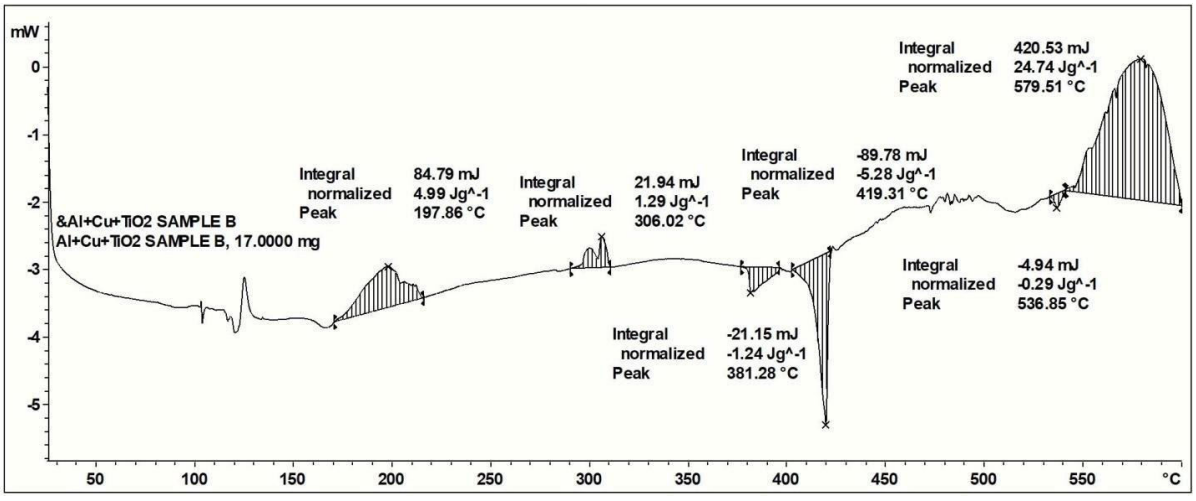

Figure 5: The DSC curve of AA 7068–2.0 wt.% Al_2O_3, TiO_2 and Cu nanocomposite powders after 30 hrs of Ball milling.

The differential scanning calorimetry used to measure enthalpy changes due to changes in the physical and chemical properties of a material as a function of temperature or time. Heat flow is directly proportional to the capacity of the material for the given temperature. The studies were conducted by using 17 mg sample in an aluminium sample holder by purging of pure nitrogen gas at an airflow rate 50 ml/min with a temperature range of 25°C to 600°C through a heating rate of10°C/min. The endothermic peak at 536.85°C corresponds to the melting of aluminium, which was followed by a steady-state exothermic reaction at 579.51°C. The higher calorific value obtained from this study was (ΔH) 24.74J/g.

3.3. Density and Hardness Measurement

Table **4** shows the density and hardness measurement of prepared nanocomposites. Theoretical density was calculated by the rule of mixture. The green and sintered densities of the prepared nanocomposites were determined to employ the Archimedes principle. The growth of the theoretical, green and sintered densities (%), significantly increased, due to the very fine particle size and distribution of reinforcements in a soft alloy matrix. Fig. (**6a-b**) shows the relation between theoretical, green and sintered densities. The density positively correlated with the reinforcement content (0%, 2% and 4%) The densities of these nanocomposites was increased after sintering. The growth of the theoretical density (%) significantly increased, due to the very fine particle size and distribution of reinforcements in a soft alloy matrix. This effect was confirmed by our earlier results (33-35). The Hardness test was conducted by the Brinell Hardness Testing Machine. The experimental error was less than 10% in the hardness measurement. The Brinell hardness number 173.2 BHN, 192 BHN and 184 BHN values were obtained for Al 7068-0 wt.% Al_2O_3, TiO_2 and Cu nanocrystalline, Al 7068-2 wt.% Al_2O_3, TiO_2 and Cu nanocomposites and Al 7068-4 wt.% Al_2O_3, TiO_2 and Cu nanocomposites respectively.

The higher amount of reinforcement (More than 2 Wt. %) will lead to particle agglomeration and deteriorate mechanical properties. Al 7068-2 Wt.%

Table 4: Density and Hardness Measurement

Sl. No	Nanocomposites	Theoretical Density (g/cc)	Actual Density (g/cc)		Brinell Hardness Number (BHN)
			Before Sintering	After Sintering	
1	Al 7068-0 wt.% Al_2O_3, TiO_2 and copper	2.85	2.62416	2.64138	173
2	Al 7068-2 wt.% Al_2O_3, TiO_2 and copper	3.02254	2.73994	2.76988	192
3	Al 7068-4 wt.% Al_2O_3, TiO_2 and copper	3.19508	2.90685	2.95462	184

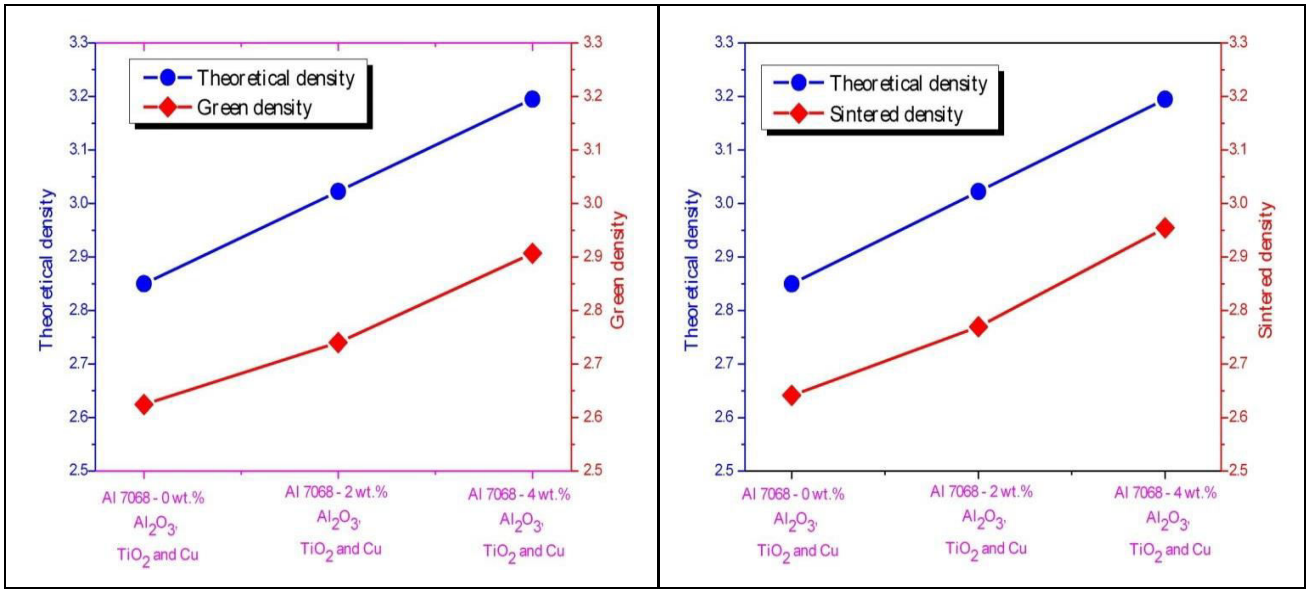

Figure 6: (a) Theoretical density Vs Green density; (b) Theoretical density Vs Sintered density.

Al2O3, TiO2 and Cu nanocomposites gave more hardness value than Al 7068 -4 Wt.% Al2O3, TiO2 and Cu nanocomposites. Because, the agglomeration of particles will lead to decrease mechanical properties. Furthermore, the addition of reinforcement content gave a reduction in hardness. Fig. (**7**) shows Brinell hardness number (BHN) of prepared AA 7068 nanocomposites after 30 hrs of MA. The 2 Wt. % of reinforcement content in metal matrix gave optimum mechanical properties and it was confirmed by previous studies [32-34].

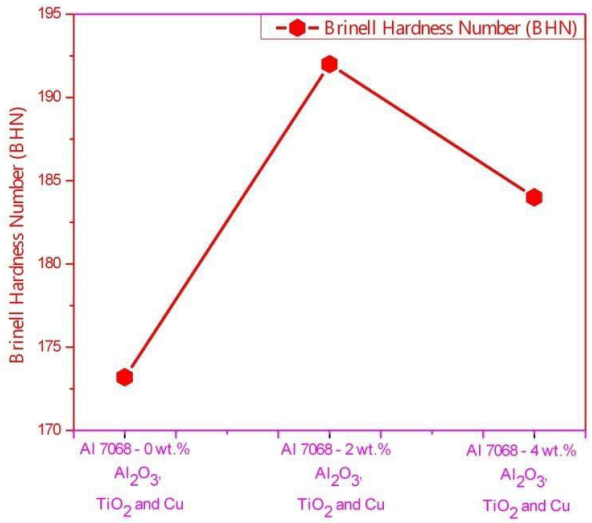

Figure 7: Brinell hardness number (BHN) of prepared AA 7068 nanocomposites after 30 hrs of MA.

4. CONCLUSION

The present study examined AA7068-xwt. % Al_2O_3, TiO_2 and Cu (x = 0 wt. %, 2wt. %, and 4wt. %) nanocomposite prepared by powder metallurgy route and synthesis, structural changes, characterization and mechanical behavior.

The powder morphology of prepared nanocomposites was investigated and reported as a function of milling time. An XRD result reveals that there are no intermetallic compounds formed in the milled powder after 30 hr of mechanical alloying. An equiaxed and almost spherical powder morphology was obtained after 30 hr mechanical alloying which was characteristic of the steady state. The reinforcement particles were well embedded and uniformly distributed in Al 7068 metal matrix composites. It was confirmed by bright-field emission transmission electron microscopy (FETEM) image and selected area diffraction (SAD) ring pattern. From the DSC curve of AA 7068–2.0 wt. % Al_2O_3, TiO_2 and Cu nanocomposite powders after 30 hrs of mechanical alloying, the endothermic peak at 536.85°C corresponds to the melting of aluminium which was followed by a steady-state exothermic reaction at 579.51°C. The higher calorific value of (ΔH) 24.74J/g. Density and hardness measurement was analyzed. Al 7068-2 wt. % Al_2O_3, TiO_2 and Cu nanocomposites gave better hardness value 192 BHN and it was 11% more than unreinforced nanocrystalline.

Densification behavior, wear behavior and tensile and compression strength measurements for the above-prepared nanocomposite materials will be analysed and addressed in future work.

REFERENCES

[1] Zhang XX. Mechanical properties of ABOw+MWNTs/Al hybrid composites made by squeeze cast technique. Mater Lett 2007;61(16):3504-06. https://doi.org/10.1016/j.matlet.2006.11.113

[2] Farman Ali, Muhammed Waseem, Rafaqat Khurshid, Adeel Afzal. TiO2 reinforced high-performance epoxy-co-polyamide composite coatings. Progress in Organic Coatings 2020;146: 105726. https://doi.org/10.1016/j.porgcoat.2020.105726

[3] Siddabathula Madhusudan, Mohammed Moulana Mohiuddin Sarcar, Narsipalli Bhargava Rama Mohan Rao. Mechanical properties of Aluminum-Copper (p) composite metallic materials. Journal of Applied Research and Technology. 2016;14 (5):293-299. https://doi.org/10.1016/j.jart.2016.05.009

[4] K.Jhon Joshua, P. Sherjin, J. Perinba Selvin Raj. The analysis of ball-milled aluminium alloy 7068 metal powders. SSRG International Journal of Mechanical Engineering (SSRG - IJME). 2017; 4 (8). https://doi.org/10.14445/23488360/IJME-V4I8P102

[5] K.Jhon Joshua, S. J. Vijay, D. Philip Selvaraj, P. Ramkumar. Influence of MgO particles on Microstructural and mechanical behaviour of AA7068 Metal Matrix Composites. Materials Science and Engineering 2017; 247: 012011. https://doi.org/10.1088/1757-899X/247/1/012011

[6] J.Lakshmipathy, S. Rajesh Kannan, K.Manisekar, S.Vinoth Kumar. Effect of reinforcement and Tribological Behaviour of AA7068 Hybrid Composites Manufactured through Powder Metallurgy Techniques. Applied Mechanics and Materials 2017; 867:19-28, 2017. https://doi.org/10.4028/www.scientific.net/AMM.867.19

[7] M. Madhusudhan, G.J.Naveen, K.Mahesha. Mechanical Characterization of AA7068-ZrO2 reinforced Metal Matrix Composites. Materials Today: Proceedings 2017: 4 (2): 3122-3130. https://doi.org/10.1016/j.matpr.2017.02.196

[8] V. Sridhar, Ch. Ratnam, M. Ashok Chakravarthy. Synthesis and Mechanical Characterization of Magnesium Reinforced With Nano Alumina Composites. Materials Today: Proceedings 2017; 4 (2); 3131-3140. https://doi.org/10.1016/j.matpr.2017.02.197

[9] Ali Hubi Haleem, Newfal Zuheir and Newal Muhammad Dawood. Preparing and Studying Some Mechanical Properties of Aluminium Matrix Composite Materials Reinforced by Al2O3 particles. Journal of Babylon University/Engineering Sciences 2012; 20 (1).

[10] M. Karbalaei Akbari, H.R.Baharvandi, and O.Mirzaee. Fabrication of nano-sized Al2O3 reinforced casting aluminium composite focusing on preparation process of

reinforcement powders and evaluation of its properties. Composites: Part B. 2013; 55: 426-432. https://doi.org/10.1016/j.compositesb.2013.07.008

[11] M. Karbalaei Akbari, H.R.Baharvandi, and O.Mirzaee. Investigation of particle size and reinforcement content on mechanical properties and fracture behaviour of A356-Al2O3 composite fabricated by the vortex method. Journal of Composite Materials. 2014; 48 (27):3315-3330. https://doi.org/10.1177/0021998313507618

[12] A.Baradeswaran and A.Elayaperumal. Study on mechanical and wear properties of Al 7075/Al2O3/graphite hybrid composites. Composites: Part B. 2014; 56:464-471. https://doi.org/10.1016/j.compositesb.2013.08.013

[13] Chen, F., Wang, T. M., Chen, Z. N., Mao, F., Han, Q. and Cao, Z. Q. Microstructure, mechanical properties and wear behaviour of Zn-Al-Cu-TiB2 in situ composites. Transactions of Nonferrous Metals Society of China. 2015; 25:103-111. https://doi.org/10.1016/S1003-6326(15)63584-1

[14] S. Dhanalakshmi, N.Mohanasundararaju and P.G. Venkatekrishnan. Preparation and mechanical characterization of stir cast hybrid Al7075-Al2O3-B4C metal matrix composites. Applied Mechanics and Materials. 2014; 92-594:705-710. https://doi.org/10.4028/www.scientific.net/AMM.592-594.705

[15] Kumar, A., Lai, S. and Kumar, S. Fabrication and Characterization of A359/Al2O3 metal matrix composite using the electromagnetic stir casting method. Journal of Materials Research and Technology. 2013; 2(3): 250-254. https://doi.org/10.1016/j.jmrt.2013.03.015

[16] Mahallawi, I.E., Shash, Y., Rashad, R.M., Abdelaziz, M.H., Mayer, J. and Schwedt, A. Hardness and wear behaviour of semi-solid cast A390 alloy reinforced with Al2O3 and TiO2 nanoparticles. Arabian Journal for Science and Engineering. 2014; 39:5171-5184. https://doi.org/10.1007/s13369-014-1179-3

[17] A. Mazahery and M.Ostadshabani. Investigation on mechanical properties of nano-Al2O3-reinforced aluminium matrix composites. Journal of Composite Materials. 2011; 45(24):2579-2586. https://doi.org/10.1177/0021998311401111

[18] Y.Sahin and K.E.Oksuz. Tribological behaviour of Al2014-Al2O3 particle reinforced composites produced by powder metallurgy method. Journal of the Balkan Tribological Association. 2013; 19(2):190-201.

[19] S.A. Sajjadi, H.R.Ezatpour, and M.T.Parizi. Comparison of microstructure and mechanical properties of A356 aluminium alloy/Al2O3 composites fabricated by stir and compo-casting processes. Materials & Design. 2012; 34:106-111. https://doi.org/10.1016/j.matdes.2011.07.037

[20] S.A. Sajjadi, M.T.Parizi, H.R.Ezatpour, A.Sedghi. Fabrication of A356 composite reinforced with micro and nano Al2O3 particles by a developed compocasting method and study of its properties. Journal of Alloys and Compounds. 2012; 511:226-231. https://doi.org/10.1016/j.jallcom.2011.08.105

[21] K. Sekar, K.Allesu and M.A.Joseph. Effect of T6 heat treatment in the microstructure and mechanical properties of A356 reinforced with nano Al2O3 particles by combination effect of stir and squeeze casting. Procedia Materials Science. 2014; 5:444-453. https://doi.org/10.1016/j.mspro.2014.07.287

[22] S. Tahamtan, A.Halvaee, M.Emamy, and M.S.Zabihi. Fabrication of Al/A206-Al2O3 nano/micro composite by combining ball milling and stir casting technology. Materials& Design. 2013; 49:347-359. https://doi.org/10.1016/j.matdes.2013.01.032

[23] K.Umanath, K.Palanikumar, and S.T.Selvamani. Analysis of dry sliding wear behaviour of Al6061/SiC/Al2O3 hybrid metal matrix composites. Composites: Part B. 2013; 53:159-168. https://doi.org/10.1016/j.compositesb.2013.04.051

[24] Mohammad Khoshghadam-Pireyousefan, Roohollah Rahmanifard, Lubomir Orovcik, Peter Svec, Volker Klemm. Application of a novel method for fabrication of graphene reinforced aluminium matrix nanocomposites: Synthesis, microstructure, and mechanical properties. Materials Science & Engineering A. 2020; 772:138820. https://doi.org/10.1016/j.msea.2019.138820

[25] Avwerosuoghene Moses Okoroa, Ronald Machakab, Senzeni Sipho Lephuthinga, Samuel Ranti Okea, Mary Ajimegoh Awotundea, Peter Apata Olubambia, Evaluation of the sinterability, densification behaviour and microhardness of spark plasma sintered multiwall carbon nanotubes reinforced Ti6Al4V nanocomposites. Ceramics International.2019; 45:19864-19878. https://doi.org/10.1016/j.ceramint.2019.06.242

[26] M.K.Akbari, S Rajabi, K Shirvanimoghaddam and H.R.Baharvandi. Wear and friction behaviour of nanosized TiB2 and TiO2 particle-reinforced casting A356 aluminium nanocomposites: A comparative study focusing on particle capture in the matrix. Journal of Composite Materials 2015;161(29):3665-3681. https://doi.org/10.1177/0021998314568327

[27] Meysam Toozandehjani, Khamirul Amin Matori, Farhad Ostovan, Sidek Abdul Aziz and Md Shuhazlly Mamat. Effect of Milling Time on the Microstructure, Physical and Mechanical Properties of Al-Al2O3 Nanocomposite Synthesized by Ball Milling and Powder Metallurgy. Materials 2017; 10(11):1232. https://doi.org/10.3390/ma10111232

[28] Yilong Yang, Zhilin Liu, Ripeng Jiang, Ruiqing Li, Xiaoqian Li. Microstructural evolution and mechanical properties of the AA2219/TiC nanocomposite manufactured by ultrasonic solidification. Journal of Alloys and Compounds 2019;811:151991. https://doi.org/10.1016/j.jallcom.2019.151991

[29] J.Osten, B.Milkereit, M.Reich, B.Yang, A.Springer, K.Nowak, O.Kessler. Development of Precipitation Hardening Parameters for High Strength Alloy AA 7068. Materials. 2020;13: 918. https://doi.org/10.3390/ma13040918

[30] Amin Azimi, Ali Shokuhfar, Omid Nejadseyfi, Hamid Fallahdoost, Saeid Salehi. Optimizing consolidation behaviour of Al 7068−TiC nanocomposites using Taguchi statistical analysis. Transaction of Nonferrous Metals Society of China.2015; 25(8):2499-2508. https://doi.org/10.1016/S1003-6326(15)63868-7

[31] R. Taherzadeh Mousavian, S. Behnamfard, R. Azari Khosroshahi, J. Zava Snik, P. Ghosh, S. Krishnamurthy, A. Heidarzadeh, D. Brabazon. Strength-ductility trade-off via SiC nanoparticle dispersion in A356 aluminium matrix. Materials Science & Engineering A 2020;771: 138639. https://doi.org/10.1016/j.msea.2019.138639

[32] K.R. Ramkumar, S. Natarajan. Tensile properties and strengthening effects of Al 3003 alloy weldment reinforced with TiO2 nanoparticles. Composites Part B 2019; 175:107159. https://doi.org/10.1016/j.compositesb.2019.107159

[33] D. Jeyasimman, S. Sivasankaran, K. Sivaprasad, R. Narayanasamy, R.S. Kambali. An investigation of the synthesis, consolidation and mechanical behaviour of Al 6061 nanocomposites reinforced by TiC via mechanical alloying. Materials and Design 2014; 57: 394-404. https://doi.org/10.1016/j.matdes.2013.12.067

[34] D. Jeyasimman, K.Sivaprasad, S.Sivasankaran, R.Narayanasamy. Fabrication and consolidation behaviour of Al 6061 nanocomposite powders reinforced by multi-walled carbon nanotubes". Powder Technology. 2014; 258:189-197. https://doi.org/10.1016/j.powtec.2014.03.039

[35] D. Jeyasimman, K.Sivaprasad, S.Sivasankaran, R.Ponalagusamy, R.Narayanasamy, Vijayakumar Iyer.

Microstructural observation, consolidation and mechanical behaviour of AA 6061 nanocomposites reinforced by γ-Al2O3 nanoparticles. Advanced Powder Technology. 2015; 26:139-148. https://doi.org/10.1016/j.apt.2014.08.016

[36] G.K. Williamson, W.H.Hall. X-ray line broadening from field aluminium and wolfram. Acta Metall 1953; 1(1):22-31. https://doi.org/10.1016/0001-6160(53)90006-6

[37] Cullity B.D. Elements of X-ray diffraction 2nd edition Addison-Wesley.London.UK.1978.

Received on 15-11-2020 Accepted on 20-12-2020 Published on 30-12-2020

DOI: https://doi.org/10.31875/2410-4701.2020.07.09